

Microscopic structure of the hydrogen-boron complex in crystalline silicon

P. J. H. Denteneer,* C. G. Van de Walle,[†] and S. T. Pantelides

IBM Research Division, Thomas J. Watson Research Center, Yorktown Heights, New York 10598

(Received 21 November 1988)

The microscopic structure of hydrogen-boron complexes in silicon, which result from the passivation of boron-doped silicon by hydrogen, has been extensively debated in the literature. Most of the debate has focussed on the equilibrium site for the H atom. Here we study the microscopic structure of the complexes using parameter-free total-energy calculations and an exploration of the entire energy surface for H in Si:B. We conclusively show that the global energy minimum occurs for H at a site close to the center of a Si—B bond (*BM* site), but that there is a barrier of only 0.2 eV for movement of the H atom between four equivalent *BM* sites. This low energy barrier implies that at room temperature H is able to move around the B atom. Other sites for H proposed by others as the equilibrium sites are shown to be saddle points considerably higher in energy. The vibrational frequency of the H stretching mode at the *BM* site is calculated and found to be in agreement with experiment. Calculations of the dissociation energy of the complex are discussed.

I. INTRODUCTION

The role that hydrogen plays in semiconductors has become the subject of intense research^{1,2} following the discovery that hydrogen is able to passivate the electrical activity of shallow acceptors in silicon. This passivation effect is of considerable importance for technological reasons. The properties of electronic devices are largely determined by the presence and activity of shallow impurity levels and passivation of their activity by omnipresent (accidentally or intentionally) hydrogen would alter the properties of those devices in an uncontrollable way as long as the passivation mechanism is not thoroughly understood. The passivation effect was first suggested by Sah *et al.*³ in an inventive analysis of experiments on metal-oxide-semiconductor (MOS) capacitors. The connection between hydrogen and boron (as the prototypical acceptor-type impurity) concentrations was soon established in studies of the passivation effect under controlled experimental conditions by Pankove *et al.*⁴ and Johnson.⁵ This discovery supplemented the understanding of the role of hydrogen in semiconductors, which was previously known to be the saturation of dangling bonds at defects, surfaces, and interfaces, or passivation of *deep* levels in the energy gap, e.g., those due to transition-metal impurities. At first, the passivation effect was found to be considerably smaller in case of silicon doped with donor-type impurities (*n* type).⁶ Recently, however, it was found that also in *n*-type material there is a strong passivation effect, although still not as strong as in *p*-type material.⁷

A large number of experiments was performed to elucidate the fundamental reactions underlying the passivation mechanism and they generally claimed to support each other. For some time, however, the analysis of these experiments contained contradictory assumptions regarding the charge state of H. A step forward in the understanding of the passivation mechanism was made in Ref. 8, in which one of the present authors suggested that hy-

drogen is a deep donor in silicon and was able to account for a large portion of the experimental observations. Assuming that H is a deep donor in Si, passivation in *p*-type material would come about in two steps: (1) compensation, i.e., the annihilation of free holes associated with the ionized acceptors by the electrons of the H atoms, and (2) formation of a neutral complex (or pair) out of a negatively charged acceptor and a positively charged H atom. We stress that the first step already establishes passivation and that the second step is only the logical consequence of the first step. On the basis of first-principles total-energy calculations, Van de Walle *et al.*⁹ conclusively showed that H indeed acts as a donor in *p*-type material, confirming the proposed passivation mechanism. This conclusion could be reached from calculations for H in different charge states in pure Si. Questions pertaining to the nature and quantitative properties of the hydrogen-acceptor complex were not addressed in that work.

Soon after the hydrogen-acceptor complexes were discovered, a controversy arose regarding their microscopic structure. Pankove *et al.*,⁴ on the basis of infrared spectroscopy of boron-doped Si (Si:B), proposed that H would be inserted in a Si—B bond with the substitutional B pushed out toward the plane of three neighboring Si atoms. This configuration was confirmed in theoretical calculations by DeLeo and Fowler,¹⁰ who used a semiempirical cluster method. These authors also reproduced the measured vibrational frequency of the H stretching mode. However, Assali and Leite,¹¹ using a method very similar to the one DeLeo and Fowler employed, proposed a site for the H atom on the extension of a Si—B bond, the so called antibonding site. Using a spring-constant model they too were able to reproduce the measured H vibrational frequency, although DeLeo and Fowler¹² found a very different frequency if H were to be at the antibonding site. Based on tight-binding-model calculations for the hydrogenated vacancy in pure Si, Baranowski and Tatarkiewicz¹³ speculated

that H would occupy a site on the extension of a B—Si bond (backbonding site), forming a Si(*p*)—H(*s*) bond. Hartree-Fock cluster calculations were used by Amore Bonapasta *et al.*,¹⁴ who found a position near the center of a Si—B bond as the equilibrium site for H.

Experimental investigations into the microscopic structure of hydrogen-acceptor complexes (in which the acceptor usually is boron) have included infrared measurements and Raman studies of the H vibrational frequency,^{4,5,15–17} ion-channeling measurements of the lattice location of H and the displacement from the substitutional site of B,^{18–21} the perturbed-angular-correlation technique to explore hydrogen-indium pairs in Si,²² x-ray-diffraction studies of the lattice relaxation due to passivation,²³ and uniaxial-stress studies of the H-stretching mode.²⁴ Generally, the picture emerges from these studies that H dominantly occupies a site near the center of a Si—B bond, although smaller percentages are seen to reside at antibonding or tetrahedral interstitial sites.^{19,20,22} The latter observations, however, could also be connected with damage induced by H. The vibrational frequency of the H-stretching mode is found to be 1903 cm⁻¹ for low temperatures^{16,17} (~5 K). We will discuss some of the results in these papers in more detail in Sec. III, where the theoretical results of the present paper are given.

In previous theoretical work^{10–14,25,26} only a limited set of possibilities for the equilibrium site of the H atom was considered. Since it is to be expected that *anytime* the H atom is located close to the B atom it will remove the electrically active level from the gap, it is necessary to study the entire total-energy surface for H in B-doped Si in order to determine the favored site. Furthermore, since the energy differences between configurations in which H occupies different sites are small, there is a need for accurate calculations of such energy differences. Most of the theoretical approaches above use either a cluster model, usually without studying the effect of enlarging the cluster or the effect of terminating the cluster in different ways, and/or semiempirical Hamiltonians that contain a number of parameters that have been fitted to reproduce the properties of *molecules*. If tests are performed one invariably finds (see, e.g., Ref. 25) that these methods are unable to reproduce the properties of even simple bulk semiconducting crystals. When the techniques are used for small clusters to simulate defects in crystals, quite often some of the results are in agreement with either experiment or more sophisticated calculations. Typically, however, other results may be in serious error. In general, the lack of tests of convergence and accuracy renders most predictions of such calculations as questionable. In this work, we use a parameter-free method of calculating total energies, the pseudopotential-density-functional method (see Sec. II), which has proven to be very reliable in calculating and predicting properties of a wide variety of semiconducting systems, such as bulk solids, surfaces, interfaces, and localized and extended defects. Furthermore, we test all of our results for convergence and accuracy with respect to numerical approximations involved. Finally, we have developed a way to visualize the entire energy surface for a H interstitial atom in B-doped Si similar to the method used by

some of the present authors in a study of H in pure Si.⁹

The remainder of the paper is organized as follows: In Sec. II we discuss calculational details of our method that are especially pertinent to the present study, as well as tests of how the results depend on the inevitable numerical approximations involved. In Sec. III the results of our approach are presented and compared with available experimental data. Finally, we summarize the paper in Sec. IV.

II. CALCULATIONAL DETAILS

The Hamiltonian in the Kohn-Sham equations²⁷ for the valence electrons in a crystal is constructed using norm-conserving pseudopotentials²⁸ to describe the interaction between atomic cores (nuclei plus core electrons) and valence electrons. For the exchange and correlation interaction we use the local-density approximation (LDA) to the exchange and correlation functional that was parametrized by Perdew and Zunger²⁹ from the Monte Carlo simulations of an electron gas by Ceperley and Alder.³⁰

We solve the Kohn-Sham equations by expanding all functions of interest (one-electron wave functions, potentials, etc.) in plane waves and solving the resulting matrix eigenvalue problem. This procedure is iterated until a self-consistent solution is obtained, i.e., until the effective potential for the valence electrons that enters the Hamiltonian equals the effective potential that is calculated from the wave functions that are solutions for this Hamiltonian. From the self-consistent one-electron energies and wave functions the total energy of the crystal is most conveniently calculated in momentum space.^{31,32} This pseudopotential-density-functional method is a “first-principles” method in that it contains no adjustable parameters derived from experiment. This method has been very successful in calculating and predicting the ground-state properties of a wide variety of semiconducting systems.³³

We calculate the total energy for a silicon crystal with a substitutional boron atom and an interstitial hydrogen atom for a large number of inequivalent sites of the H atom. For every position of the H atom that we consider, the atoms of the Si:B host crystal are allowed to relax by minimizing the total energy with respect to the host-crystal atomic coordinates. Relaxations up to second-nearest neighbors are investigated as to their importance.

As the method in general is well documented, we will discuss only the calculational details that are especially pertinent to the present study.

A. Norm-conserving pseudopotentials

For Si and B norm-conserving pseudopotentials are generated according to the scheme of Ref. 28. We use the degrees of freedom that one has in generating such pseudopotentials to our advantage by carefully choosing core cutoff radii r_c (outside of which true and pseudo-wave-functions are identical²⁸). These cutoff radii can be chosen such that a pseudopotential is generated whose Fourier transform converges more rapidly in q space, implying that a smaller number of plane waves will be re-

quired to describe the pseudopotential.³⁴ Generally, moving r_c outward improves the pseudopotential in the above respect. However, moving r_c outward deteriorates the description of the atom by the pseudopotential. Cutoff radii are chosen such that a reasonable balance between both effects is found. The Si pseudopotential is the same as used in previous work and is described elsewhere.^{9,35} The pseudopotential for B is newly generated and is discussed here in more detail. We generate pseudopotentials for angular-momentum components $l=0$ and 1 only. The cutoff radii for $l=0$ and 1 are 1.10 and 1.18 a.u., respectively. These r_c are somewhat larger than those used in Ref. 36 (1.0 and 0.9 a.u. for $l=0$ and 1, respectively). The generated pseudopotential is tested by calculating the equilibrium lattice constant a_{eq} and bulk modulus B_0 of boron phosphide (BP) in the zincblende structure for consecutively larger values of the kinetic-energy cutoffs E_1 and E_2 , which determine the numbers of plane waves in the expansion of the wave functions (plane waves with kinetic energy up to E_2 are included in the calculation, those between E_1 and E_2 in second-order Löwdin perturbation theory;³⁷ we invariably choose $E_2=2E_1$). In the following, we will use the notation $(E_1;E_2)$ to denote the choice of cutoffs. The calculations are performed both for the newly generated B pseudopotential as well as for the one that is tabulated in Ref. 38. For phosphorus we use in both cases the tabulated pseudopotential of Bachelet, Hamann, and Schlüter³⁸ (to be called the BHS pseudopotential). The Fourier transform of the P pseudopotential falls off more rapidly for large q than the Fourier transform of the B pseudopotential. Therefore the convergence with respect to kinetic-energy cutoff will be determined by the B pseudopotential. For each choice of energy cutoffs, a_{eq} and B_0 are calculated by computing the total energy of BP at five lattice constants ranging between -5% and $+5\%$ of the experimental lattice constant.³⁹ The results are fitted to Murnaghan's equation of state for solids, which contains a_{eq} and B_0 as parameters.⁴⁰

We combine the results for a_{eq} and B_0 in Fig. 1. The single points in Fig. 1 ($a_{\text{eq}}=4.56$ Å and $B_0=1.66$ Mbar) are results obtained in Ref. 36 using a pseudopotential for B and P very much like the BHS pseudopotential and an energy cutoff of 20 Ry (no Löwdin perturbation technique was used in their calculation). Our results indicate that the results of Ref. 36 have not entirely converged with respect to increasing the energy cutoff. The main conclusion to be drawn from Fig. 1 is that the newly generated B potential results in virtually the same a_{eq} and B_0 as found with the BHS pseudopotential, but that it converges faster to these values than with the BHS pseudopotential. Both converged values for a_{eq} (4.48 and 4.49 Å for the new and BHS pseudopotential, respectively) are in fair agreement with the lattice constant of 4.538 Å that is found experimentally.⁴¹ The calculated bulk moduli of 1.62 and 1.68 Mbar for the new and BHS pseudopotential, respectively, cannot be compared with any experimental result. Therefore, we have reached our goal of generating a norm-conserving pseudopotential that can be represented by fewer plane waves than the one so far

available, while it still accurately describes a B atom in a solid-state environment.

To illustrate the point that the cutoff radii r_c cannot be pushed out too far, we mention that the converged result for a_{eq} using a potential for B generated by choosing the r_c to lie at radii for which the outermost maxima of the radial wave function for the respective l values occur ($r_c=1.52$ and 1.56 a.u. for $l=0$ and 1, respectively) is 4.34 Å. The percentage of deviation from the experimental value is more than 3 times as large as for the two other pseudopotentials.

For hydrogen we did not use a pseudopotential, although it is possible to generate one. Instead we use the

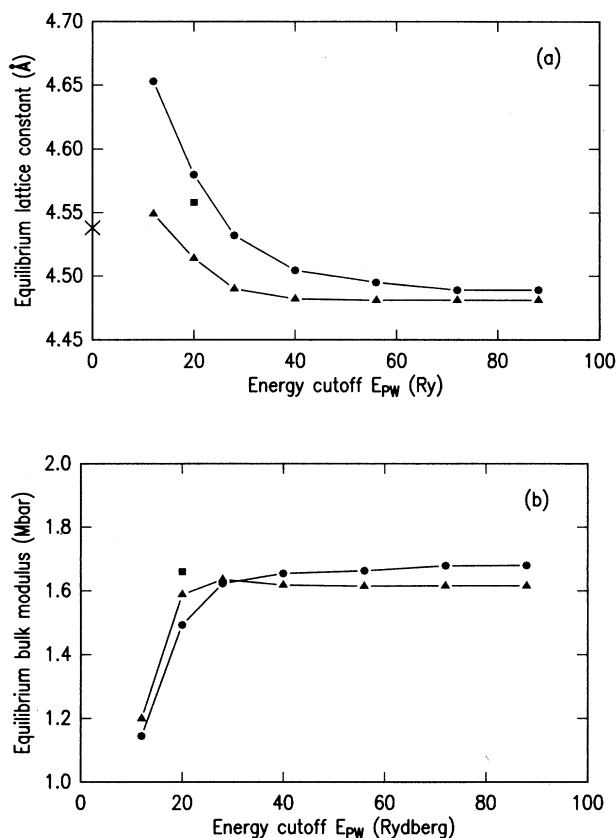


FIG. 1. Convergence of ground-state properties of BP as a function of kinetic energy cutoff E_{PW} (determining the number of plane waves in the expansion of the wave functions) for two different pseudopotentials for boron. The dots represent results obtained using the tabulated pseudopotentials for B and P from Ref. 38, whereas the triangles represent results obtained using a newly generated pseudopotential for B and the tabulated pseudopotential from Ref. 38 for P. The solid squares represent results obtained in Ref. 36 using pseudopotentials for B and P very similar to the pseudopotentials in Ref. 38. Plane waves with kinetic energy up to $\frac{1}{2}E_{\text{PW}}$ are included exactly in the calculation, and those between $\frac{1}{2}E_{\text{PW}}$ and E_{PW} in second-order perturbation theory (Ref. 37). (a) Equilibrium lattice constant a_{eq} of BP (in Å). The cross on the vertical axis denotes the experimental lattice constant (Ref. 41). (b) Equilibrium bulk modulus B_0 of BP (in Mbar).

exact $1/r$ Coulomb potential of the proton. In this we follow our earlier work^{9,35} and we refer to those papers for a more detailed discussion.

We note that Fig. 1 is not instrumental in determining the energy cutoffs that will be sufficient for the problems to be addressed in this paper. Those cutoffs depend on the properties and accuracy one is interested in and can only be determined by explicitly calculating those properties for consecutively larger cutoffs. This will be discussed in more detail in Sec. IID. Figure 1 *does* show qualitatively that these properties may be obtained at lower cutoffs by using the newly generated B potential as compared to the (standard) BHS pseudopotential.

B. Supercells

To model simple and complex defects we use supercells that are periodically repeated. We investigate how calculated properties depend on supercell size and we determine when they become independent of supercell size (within a desired accuracy). As in previous work^{9,35,42} we use supercells of 8, 16, and 32 atoms in which defects are separated by 5.43, 7.68, and 9.41 Å, respectively.

In addition to the finite separation between defects, another artifact particularly pertinent to defect calculations in general arises from using a (finite-size) supercell. Defect levels that show no dispersion for a truly isolated defect do have dispersion when using finite-size supercells. This is, however, not a big problem in the present calculation. The substitutional B and interstitial H atoms together exactly supply the four valence electrons of the Si atom that has been replaced by the substitutional B atom. Therefore an equal number of bands is filled as in the case of pure Si. Therefore, a H-related defect level, which is found to be located in the energy gap exactly as in the case of H in pure Si (See Ref. 35 and also Sec. III A) is unoccupied. Even if a large dispersion of this level causes it to drop into the valence bands for certain points in the first Brillouin zone (1BZ), the level can be left unoccupied when it is properly identified [this identification can be done in a variety of ways: (1) the charge density associated with the defect level is localized and correlated with the position of H; (2) by comparing the band structure of Si with a substitutional B atom (Si:B) with and without the H atom; (3) the H-related defect level will move significantly with respect to the other bands if the band structure is calculated with the H atom at a different position].

The dispersion of the H-related defect level for H in Si:B is about 2.0, 1.1, and 0.6 eV for the 8-, 16-, and 32-atom cells, respectively. See Sec. III A for a further discussion of these levels.

C. Brillouin-zone integrations

In two distinct stages of the calculation of the total energy, an integration over the 1BZ has to be performed: (1) calculation of the valence charge density from the one-electron wave functions, and (2) calculation of the band-structure energy term from the one-electron energies.³² Both integrations are replaced by summations

over special \mathbf{k} points in the irreducible part of the 1BZ (IRBZ).^{43,44} It has been established in many calculations that by using only a very small number of \mathbf{k} points (between 1 and 10) very accurate total-energy *differences* can be obtained. In general, one has to test for every application how many \mathbf{k} points are sufficient for a certain accuracy. Such tests are reported below.

We employed the general Monkhorst-Pack (MP) scheme⁴⁴ to generate special points sets with their parameter q equal to 2. The number of special points generated with this choice of q depends on the position of the H atom in the unit cell. It is also different for the different supercell sizes that we use. When H is located at a general position on the extension of a Si—B bond, $q=2$ results in two, five, and two special points for the 8-, 16-, and 32-atom cell, respectively. For less symmetric H positions this number can be as high as 16 in the 16-atom cell and 4 in the 32-atom cell. The following test was executed to determine the accuracy that is obtained with the $q=2$ choice for special points in the MP scheme: We calculate the total-energy difference between configurations in which H occupies a position near the center of a Si—B bond and one in which H is located on the extension of a Si—B bond. These two reference configurations are defined only for the purpose of carrying out meaningful tests of the Brillouin-zone integrations (this subsection) and the dependence of results on supercell size and basis-set size (next subsection). They should not be confused with the fully relaxed configurations that will be described later. In the first configuration [to be called the bond-minimum (*BM*) reference configuration] the H atom and the Si and B atoms constituting the bond in which H is located are allowed to relax their position in order to find the minimum-energy configuration. In this *BM* reference configuration the Si and B atoms relax outward by 0.24 and 0.42 Å, respectively. In the second configuration [to be called the antibonding (*AB*) reference configuration] only the H and B atoms are relaxed. In this configuration the H atom has a distance of 1.32 Å from the B atom, which relaxes inward (away from H and towards a Si atom) by 0.09 Å. The relaxation of B is an artifact springing from the fact that the Si atoms are kept fixed. In the fully relaxed *AB* configuration the four Si neighbors of B relax inward because of the smaller size of the B atom (see Sec. III B). Although we do not allow all atoms to relax, these reference configurations are certainly sufficiently close to the fully relaxed configurations to make tests meaningful. In the 16-atom cell using energy cutoffs $(E_1; E_2)=(6; 12)$ Ry, we find an energy difference of 0.316 eV for $q=2$. By choosing $q=4$, we enlarge the number of \mathbf{k} points in the 1BZ by a factor of 8 and find 30 special points in the IRBZ. For $q=4$ the above energy difference drops to 0.306 eV. In the 32-atom cell we obtain an energy difference of 0.287 eV using $q=2$ (two points in the IRBZ), whereas $q=4$ (15 points in the IRBZ) yields 0.286 eV. We conclude that the $q=2$ choice is good enough to give energy differences between configurations with different H positions and different relaxations with an accuracy of about 0.01 eV. This is slightly better than in the earlier work on H in pure Si,³⁵

since here we always integrate over a set of completely filled states. Finally, in the 8-atom cell the $q=2$ choice is not as good as in the 16- and 32-atom cells. Tests show that $q=4$ (10 points in the IRBZ) provides the same accuracy as $q=2$ in the larger cells. The 8-atom cell, however, will only be used to test the convergence of energy differences with respect to increasing the energy cutoffs (see next subsection). For that purpose the $q=2$ choice is sufficient.

D. Energy cutoffs and supercell size

Calculations using the pseudopotential-density-functional method and a plane-wave basis set are generally performed with a choice of energy cutoffs ($E_1; E_2$) for which calculated results still depend on this choice (E_2 is the kinetic-energy cutoff for plane waves included in the calculation; those with kinetic energy between E_1 and E_2 are included using second-order Löwdin perturbation theory³⁷). For a given accuracy the size of the computational problem (i.e., rank of matrices to be diagonalized) is proportional to the volume of the unit cell, whereas processing time and memory usage are cubic and quadratic, respectively, in these sizes. Only for very small unit cells the usual computational limitations (central-processor-unit time and memory usage) allow one to fully converge the calculations with respect to increasing E_1 and E_2 . One therefore has to make a careful study of the dependence on cutoffs in order to come to a judicious choice and quantitatively reliable results.

As indicated in Sec. II A, the choice of supercell size can also affect calculated energies, because if defects in neighboring cells are too close one is modeling a system with interacting defects. Here we present a study of the dependence on energy cutoffs and supercell size of the energy difference between the *BM* and *AB* reference configurations described in the preceding subsection. Table I and Fig. 2 show the results. In Fig. 2 we see that the three curves for the three supercell sizes are very well

TABLE I. Energy difference (in eV) between situations in which hydrogen occupies the bond-minimum (*BM*) and anti-bonding (*AB*) reference configurations (see text) as a function of energy cutoffs ($E_1; E_2$) in (Ry) and as a function of number of atoms in the supercell. The results for the 8-atom cell are only used to study the dependence on energy cutoff since they have not been fully converged with respect to enlarging the mesh used in the *k*-space integrations (see text).

$(E_1; E_2)$ (Ry)	8 atoms	16 atoms	32 atoms
(6;12)	0.481	0.316	0.287
(8;16)	0.518	0.358	0.333
(10;20)	0.554	0.399	0.370
(12;24)	0.586	0.433	0.400
(14;28)	0.602	0.451	
(16;32)	0.607	0.471	
(18;36)	0.610	0.475	
(20;40)	0.615		
(22;44)	0.621		
(24;48)	0.625		
(26;52)	0.628		

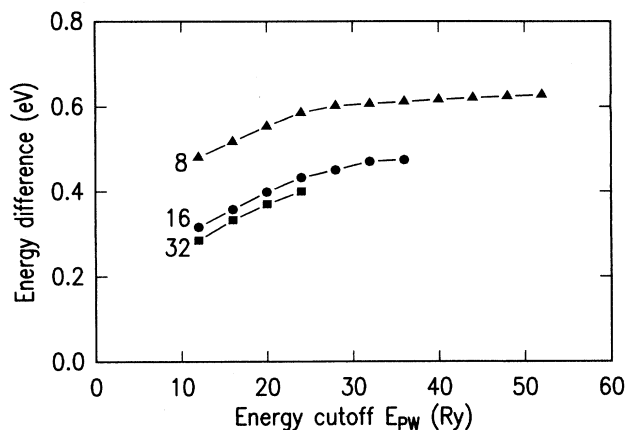


FIG. 2. Convergence of energy difference between the *BM* and *AB* reference configurations (see text) in which H occupies two different sites close to substitutional B in Si, as a function of kinetic-energy cutoff E_{PW} (see caption of Fig. 1) and of supercell size. Supercells used contain, besides the H atom, 8, 16, or 32 host-crystal atoms. The results for the 8-atom cell are only used to further probe the dependence of the energy difference on E_{PW} and are not fully converged with respect to enlarging the mesh used in the *k*-space integrations (see text).

behaved; they have the same (regular) form and are merely shifted with respect to each other by an almost constant amount. The curves for 16- and 32-atom cells do not differ by more than 0.03 eV. The 8-atom-cell curve shows that the behavior as a function of cutoff is the same as for the larger cells and convergence is eventually reached. The 8-atom-cell curve is not converged with respect to the number of *k* points used in the Brillouin-zone integrations ($q=2$ was used; see preceding subsection), which is unimportant for the present purpose of testing the dependence of energy differences on energy cutoff. For $E_2=36$ Ry we consider the energy difference to be converged, since the changes resulting from using higher cutoffs are very small compared to other numerical approximations employed (e.g., the Brillouin-zone integrations described in the preceding subsection).

We further study the energy-cutoff dependence of calculated energy differences by examining a larger set of positions for the H atom. The different sites considered here lie in the (110) plane and are depicted in Fig. 3. We use the 32-atom cell and all atoms up to second-nearest neighbors of the H atom are allowed to relax. In addition, the Si neighbors of the B atom are always allowed to relax. Table II summarizes the results. For the purpose of discussing Table II and following results, we find it useful to subdivide the different positions for the H atom into three regions. In region I the valence-electron density is very high (e.g., the *BM* site) and putting a H atom there will induce large relaxations of the crystal. In region II the electron density is lower but still considerable (e.g., the *AB*, *BB*, *C*, and *C'* sites); consequently, relaxations of the crystal are also still considerable. In region III the electron density is very small (*T_d* and *H'* sites) and the H atom will not induce much relaxation. Of course, one always has the relaxation of the Si neighbors of the B atom because of the smaller size of the B atom.

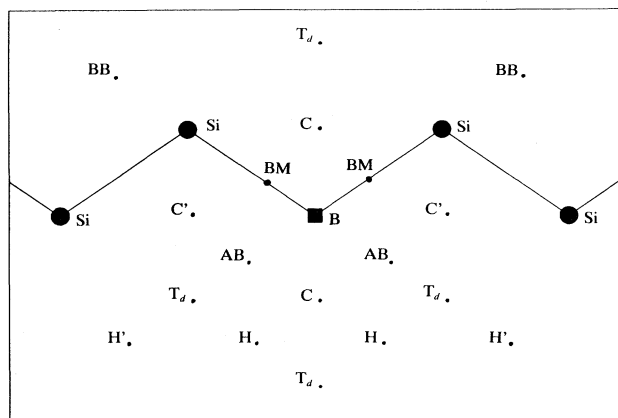


FIG. 3. Location in the (110) plane, containing a zig-zag chain of Si atoms and a substitutational B atom, of sites often referred to in the text. *BM* denotes the bond-minimum site, *AB* the antibonding site, *BB* the backbonding site, T_d the tetrahedral interstitial site, and *H* and H' are (inequivalent) hexagonal interstitial sites. The *C* and C' sites are equivalent in pure Si, but not in the presence of a substitutational B atom.

Regarding convergence with respect to increasing the energy cutoffs, we make the following observation: energy differences between sites in the same region change by less than 0.05 eV by going from cutoffs (6;12) Ry to cutoffs (10;20) Ry and therefore may be considered fairly well converged at (6;12) Ry. In these calculations the relaxations are determined at the lower cutoffs and kept fixed for the higher cutoffs so that variations of energy differences are due solely to the change in cutoffs. Energy differences between sites in different regions change by about 0.1 eV when the combination of sites is region I–region II. This observation is useful if one wants to extrapolate calculated energy differences to very high energy cutoffs, which because of computational limitations cannot be handled together with large supercells. Tables I and II together provide means of extrapolating to higher cutoffs in order to obtain reliable quantitative estimates for energy barriers. We observe from Table I that the amount of change in going from cutoffs (6;12) Ry to

TABLE II. Energies (in eV) of situations in which hydrogen occupies different sites (see text and Fig. 3) in Si:B as a function of energy cutoffs ($E_1; E_2$). As the zero of energy, the energy of the global energy minimum (*BM* site) is chosen. Energies are calculated in a 32-atom cell including relaxation up to second-nearest neighbors of the hydrogen atom. δ is the difference between the (6;12)- and (10;20)-Ry calculations.

Site	(6;12) Ry	(10;20) Ry	δ (eV)
<i>BM</i>	0.00	0.00	0.00
<i>AB</i>	0.26	0.37	0.11
<i>BB</i>	0.97	1.10	0.13
<i>C</i>	0.11	0.20	0.09
C'	1.36	1.44	0.08
H'	1.06	1.26	0.20
T_d	1.61	1.85	0.24

cutoffs (10;20) Ry is about the same as that of going from (10;20) Ry to the converged values that we consider reached at (18;36) Ry. Therefore, calculations of energy differences between two sites at (6;12) and (10;20) Ry allow one to extrapolate to the converged energy differences. Using Table II we find that the *BM* site is 0.48 eV lower than the *AB* site and 0.29 eV lower than the *C* site. One should not apply such extrapolations to energy differences between sites in regions I and III (e.g., *BM* and T_d sites) before a table like Table I for sites in regions I and III is calculated.

Considering the above results, we come to the following choice of supercell size and energy cutoffs that we will use to calculate total energies for a large number of different H positions: We use 32-atom cells and energy cutoffs of (6;12) Ry. The use of the 32-atom cell allows us to take relaxations up to second-nearest neighbors of the H atom into account. Furthermore, the (artificial) dispersion of the H-related defect level in the gap is manageable, although a larger dispersion is not a big problem for the neutral H-B pair in Si as discussed in Sec. II B. The energy cutoffs (6;12) Ry are large enough to obtain qualitatively correct energy differences between different positions of the H atom, whereas it is still possible to calculate energies for a large number of different positions, including those that destroy all point-group symmetry of the system. It is necessary to calculate the energy for a large number of different H positions to get a picture of the entire energy surface for H in Si:B. For cases of special interest the energy difference can also be found in a *quantitatively* reliable way by using higher cutoffs and extrapolation, as shown above.

Occasionally, for positions of H for which the system has very low symmetry, the total-energy difference with a position for which the system has higher symmetry, but that lies in the same density region, is calculated in a 16-atom cell. This difference is then assumed to be the same in the 32-atom cell.

E. Energy surfaces

It is very illuminating to combine the results of total-energy calculations for different positions of an impurity atom in a host crystal into an energy surface $E(\mathbf{R}_{\text{imp}})$ with the position of the impurity atom \mathbf{R}_{imp} as the coordinate (note that this does not exclude the possibility that the host crystal contains other impurities). Such a surface provides immediate insight in the migration pathways, migration barriers, and stable sites for the impurity atom.

Quite generally, the observation can be made⁹ that the function $E(\mathbf{R}_{\text{imp}})$ has the complete symmetry of the host crystal (without the tracer impurity), i.e., for any operation \mathcal{R} of the space group of the host crystal structure, we have

$$E(\mathbf{R}_{\text{imp}}) = E(\mathcal{R}\mathbf{R}_{\text{imp}}). \quad (1)$$

For instance, in a pure Si crystal, positions \mathbf{R}_{imp} of a H atom in the center of different Si—Si bonds will render the same total energy, if all the appropriate relaxations are taken into account. Of course, different atoms relax for different bond-centered (BC) sites, since the Si atoms

forming the bond in which the H atom resides will relax most strongly. However, the relaxations for two different BC sites are connected by the same symmetry operation that connects the two sites. To obtain the energy surface $E(\mathbf{R}_{\text{imp}})$ we now proceed as follows: The function $E(\mathbf{R}_{\text{imp}})$ is expanded in a basis set of functions that all have the symmetry of the host crystal. The expansion coefficients are obtained by a least-squares fit to calculated values $E(\mathbf{R}_{\text{imp},i})$ for different positions $\mathbf{R}_{\text{imp},i}$ ($i = 1, \dots, N$). By varying the degree to which the problem is overdetermined (where overdetermined means that the number of calculated data points, N , is larger than the number of symmetry functions, M , in the expansion), one can check the stability and, thus, the reliability of the fit.

For host crystals with a high degree of translational symmetry, a suitable set of basis functions is the set of symmetrized plane waves $\Phi_l(\mathbf{r})$:

$$\Phi_l(\mathbf{r}) = \sum_{m=1}^{N_l} e^{i\mathbf{K}_m^{(l)} \cdot \mathbf{r}}, \quad (2)$$

where the $\mathbf{K}_m^{(l)}$ are vectors of the reciprocal lattice that corresponds to the Bravais lattice of the crystal. For each l , the N_l vectors $\mathbf{K}_m^{(l)}$ transform into each other under operations of the crystallographic point group.

In previous work on H in pure Si,^{9,35} typically eight symmetrized plane waves and 10 calculated points $E(\mathbf{R}_{\text{imp},i})$ were sufficient to obtain stable energy surfaces. However, for the problem we are addressing in this paper, the behavior of a H atom in a boron-doped Si crystal, the translational symmetry is essentially lost, and symmetrized plane waves are a less obvious choice of basis functions for the expansion of the energy surface. A possible solution to this problem would be to add a set of localized functions, e.g., Gaussians centered on the atoms, to the basis set or use a basis set consisting completely of localized functions. The disadvantage of such an approach is that a more complicated (nonlinear) fitting problem is encountered, since also the decay constants that appear in the Gaussians need to be fitted. We have chosen the following approach: In the same spirit as used in the supercell approach discussed in Sec. II B, we use as basis functions for the expansion of the energy surface symmetrized plane waves of a supercell. In this way, periodicity is restored so that symmetrized plane waves are suitable basis functions, but the repeat distances can be chosen so large that the region around the substitutional impurity atom that we are interested in is not affected by impurities in neighboring cells. By studying the behavior of the total energy when the H atom is moved away from the B atom, and comparing this with the case of H^+ in pure Si, we establish (see Sec. III C) that the influence of the B atom has disappeared at a distance of about 2.1 Å from the B atom. Therefore, to describe the energy surface around a B atom, it is allowed to assume that it has the symmetry of the 8-atom supercell, which has repeat distances of 5.43 Å in three perpendicular directions. This, in turn, implies that the symmetrized plane waves $\Phi_l(\mathbf{r})$, with $\mathbf{K}_m^{(l)}$ reciprocal-lattice vectors belonging to the (simple-cubic) lattice of the 8-

atom cell, are suitable functions to expand the surface in. We would like to stress that this choice of supercell is independent of the choice of supercell one uses in calculating the total energies $E(\mathbf{R}_{\text{imp},i})$. For the latter purpose one needs supercells of 32 atoms to take into account all relevant relaxations of the host crystal, as argued before.

Using this approach, the total energy still has to be calculated for a large number of different positions $\mathbf{R}_{\text{imp},i}$ of the H atom. We have found that about 40 inequivalent sites in the 8-atom cell are needed to get a good description of the energy surface. This number is consistent with the number of points (ten) typically used in fitting the energy surface for H in pure Si, the diamond structure of which has a unit cell 4 times as small. Typically, 25 symmetrized plane waves are used in the fit of the energy surface of H in Si:B. Results of this procedure will be shown below.

III. RESULTS AND DISCUSSION

A. Electronic structure

The band structure for the Si crystal with the H-B complex closely resembles that of Si with a substitutional B atom; there is no acceptorlike level in the gap showing that the acceptor is passivated. We note that a supercell calculation of the band structure of Si with a substitutional B atom, but without the H atom, will only produce an acceptorlike level in the gap if very large supercells are used. The hydrogenic state corresponding to such a shallow level is known to extend over several tens of angstroms and can therefore not be described by small supercells. Indeed, we do not find such a level in calculations without the H atom with supercells of up to 32 atoms. We do find a level near the gap that behaves almost identically to the level found in the case of H in pure Si;³⁵ this level is therefore related to H. We find that the wave function associated with this level is mostly localized around the position of the H atom and that the position of this level in the gap moves when the H atom is moved. As already discussed in Sec. II B, we note that our use of supercells induces defect levels to have dispersion. To obtain a dispersionless level from our calculations, we take a weighted average of the defect-level position over the special \mathbf{k} points for which the band structure is calculated during the total-energy calculation (more symmetric \mathbf{k} points carry less weight because they map onto fewer points in the 1BZ). The position of this level depends on the location of the H atom and roughly two cases may be distinguished. If the H atom is in one of the regions of high or intermediate electron density (regions I and II as defined in Sec. II D), the H-related defect level is located slightly above the bottom of the conduction bands. If the top of the valence bands is chosen as the zero of the energy scale, the bottom of the conduction bands of Si with one substitutional B atom is found to be at 0.46 eV (an underestimation of the experimental energy gap of 1.17 eV as is usual in LDA calculations). For H at the BM , AB , C , and C' sites (see Fig. 3), the defect level is at 0.50, 0.56, 0.62, and 0.53 eV, respectively. If the H atom is in the low-density region (region III), the defect level appears as a resonance slightly below the top

of the valence bands. For H at the T_d and H' sites of Fig. 3, the defect level is at -0.37 and -0.09 eV, respectively. If the H atom is located in region III, it is not bound to any atom and acts as an acceptor. The position of the defect level is sensitive to the energy cutoffs used; the quoted results were obtained using 32-atom cells and cutoffs of (6;12) Ry and have only qualitative value. One should also bear in mind here that it is a well-known deficiency of the LDA that, while the valence bands of a semiconductor are well described, the conduction bands, and also conduction-band-related levels, are not in agreement with experiment. This problem has recently been overcome for bulk solids by including many-body corrections.⁴⁵ Since for defect calculations this solution involves a prohibitive computational effort, it has not yet been applied to such calculations, which are already very demanding by themselves.

In the self-consistent calculation of the total energy, the H-related level is always unoccupied, since the substitutional B and interstitial H atoms together exactly supply the four valence electrons of the Si atom that has been replaced by the B atom, so that only the "pure-Si"-like bands are occupied if the defect level is in the conduction bands. If the defect level is just below the top of the valence bands, it is still left unoccupied, since for the k points at which the band structure is calculated during the self-consistency process the defect level usually lies between the valence- and conduction-band levels. If it lies below the top valence-band level, we leave it unoccupied artificially to obtain a consistent comparison with the total-energy calculations for H at the other sites.

B. Relaxation of the host crystal

In this subsection we present results for the relaxation of the host crystal (Si:B) for some characteristic positions of the H atom. For every position the total energy is minimized with respect to the positions of the atoms in the host crystal.

We first mention that in the absence of the H atom the four Si neighbors of the B atom relax toward the B atom in a "breathing-mode"-type relaxation, whereas the B atom shows a very slight tendency to become threefold coordinated by moving towards a plane with three Si neighbors (it moves less than 0.1 Å). Both for neutral B (B^0) and negatively charged B (B^-) the relaxation of the Si neighbors is 0.21 Å, reducing the Si—Si bond distance of 2.35 Å by 9%. The energy gain of this relaxation is 0.9 eV. The relaxation results in a Si—B distance of 2.14 Å, which is very close to the sum of covalent radii of Si and B (1.17 and 0.90 Å, respectively). It is interesting to compare this result for the Si—B distance with an experimental result from x-ray-diffraction measurements of the lattice contraction in B-doped Si. To make the comparison, some assumptions have to be made, the validity of which is not easily assessed. We first assume that the lattice contraction is solely caused by the difference in covalent radii of Si and B (in general, there is also a, possibly competing, electronic contribution caused by the pressure dependence of the band-gap edges⁴⁶). Using our result of 2.14 Å for the Si—B distance and following the simple argument of Shih *et al.*,⁴⁷ the "natural-bond" length

defined in Ref. 48 for a Si—B bond becomes 2.07 Å. If we now use Vegard's law for the average bond length in B-doped Si (with pure Si and "zinc-blende" BSi as extreme structures), we may extract the contraction coefficient β , defined by

$$\Delta a/a = \beta C_B, \quad (3)$$

where C_B is the boron concentration and $\Delta a/a$ is the relative change in average lattice constant. We find $\beta = -4.8 \times 10^{-24}$ cm³/atom, which is in agreement with the experimental results of $\beta = -(6 \pm 2) \times 10^{-24}$ cm³/atom (see the references in Ref. 23).

The relaxation of the host crystal in the presence of a H atom is most appreciable if H resides in the BM site (see Fig. 3). This site is located in a Si—B bond slightly displaced from the bond center toward the B atom. We distinguish it from the geometrical bond center (BC), which was found to be the global energy minimum for H^+ in Si in previous work.⁹ The BM site is the global energy minimum for H in Si:B (see the next subsection). For H at this site the neighboring Si and B atoms relax outward (as measured from their ideal lattice positions) by 0.24 and 0.42 Å, respectively. The smaller outward relaxation of the Si atom is easily explained by the fact that it would relax inward by 0.21 Å if the H atom was absent. Put differently, the above relaxations allow for close to ideal H—Si and H—B distances since they result in a H—Si distance of 1.65 Å and a H—B distance of 1.36 Å. For comparison, we mention that for H^0 (H^+) in the BC site in pure Si the two Si atoms forming the bond relax outward by 0.45 Å (0.41 Å), resulting in a H—Si distance of 1.63 Å (1.59 Å). Typical H—B distances in B_2H_6 (diborane) are 1.20 Å for H in a terminating bond and 1.34 Å for H in a bridging bond.⁴⁹ The second-nearest Si neighbors of the H atom in the BM site relax outward along the original bond axes by 0.05 Å if they are bonded to the Si neighbor of H and relax inward along the original bond axes by 0.14 Å if they are bonded to the B neighbor of H. These relaxations result in Si—Si and Si—B bond distances of 2.33 and 2.11 Å, respectively, which are very close to the Si—Si distance in pure Si (2.35 Å) and the Si—B distance in Si:B (2.14 Å). The gain in energy of these relaxations compared to the configuration in which H occupies the exact bond-center site and all other atoms occupy their ideal lattice positions is calculated to be 3.2 eV.

Our calculated relaxed configuration for the BM site is in qualitative agreement with the results of previous work using a variety of methods.^{10,14,26} Notable differences are as follows. In Ref. 14 the H atom was found to reside closer to Si than to B. The outward relaxation of the B atom of 0.58 Å found by DeLeo and Fowler¹⁰ (which we extract from their Fig. 1) significantly exceeds our result of 0.42 Å, which, in turn, is larger than the experimental result of 0.28 ± 0.03 Å from ion-channeling measurements.¹⁹ The error estimate of the experimental value results from the analysis of the data and does not include the inherent insensitivity of the channeling method, which is about 0.1 Å.¹⁸

For H at the AB site (see Fig. 3), which is a minimum along the $\langle 111 \rangle$ axis, but a saddle point of the entire en-

ergy surface (see next subsection), the H—B distance is 1.32 Å. The B atom hardly moves from its substitutional site (less than 0.05 Å towards H) and the three Si neighbors relax toward B by 0.14 Å. Our calculated H—B distance is in between those found in Refs. 10 and 11, where very different distances of 1.19 and 1.8 Å, respectively, were found using similar semiempirical cluster calculations.

If H is positioned at the *C* site (Fig. 3), the B atom does not move from its substitutional site. This may again be explained by the fact that the H—B distance in this case is close to ideal (1.36 Å). Note that this is different from the case of H⁺ in pure Si, where the distance is smaller than the ideal H—Si distance of ~1.6 Å. In that case an appreciable relaxation of the Si atom away from the H atom results. For H at the *C* site in Si:B, the inward relaxation of the two Si atoms bonded to B and next to H (see Fig. 3) is obstructed by the presence of H and is only 0.05 Å, whereas the two Si atoms bonded to B but far away from H (in the plane perpendicular to that of Fig. 3) have the same inward relaxation as for the *BM* and *AB* sites discussed above. The minimum energy for H along the line connecting the *C* site and the B substitutional atom is not at the *C* site, but slightly displaced (0.24 Å) from it toward the B atom. For that position the B atom *does* relax away from the H atom to restore the preferred H—B distance of 1.36 Å.

Finally, if H is put at the tetrahedral interstitial site (*T_d*) or hexagonal interstitial site (*H* or *H'* in Fig. 3) the only relaxation is a “breathing-mode” relaxation of 0.21 Å of the Si atoms bonded to the B atom. This is exactly the same relaxation as in the complete absence of the H atom (see above), which is consistent with the earlier finding⁹ that there is no appreciable relaxation for H at the *T_d* or *H'* sites in pure Si.

From the results of first-principles total-energy calculations presented here, it can be inferred that the relaxations of the host crystal are roughly determined by the tendency of two neighboring atoms to be separated by some preferred distance. The preferred distance is roughly determined by the sum of covalent radii (for H a covalent radius of 0.43 Å has to be used). However, there are also deviations from this general behavior, e.g., the H-obstructed relaxation of two Si neighbors of B for H at the *C* site. In any case, the examples described above can be considered as a data base to allow for an efficient search for the configurational energy minimum for an arbitrary H position.

C. Energy surface for H in Si:B

The effect of introducing a substitutional boron impurity in the silicon crystal on the behavior of H is clearly demonstrated in Fig. 4. We compare the energy of a H atom in Si:B with the energy of a positively charged H (H⁺) atom in pure Si for various positions of the H atom along the line connecting two bonded Si and B atoms (two Si atoms in the case of pure Si). We note that with H⁺ in pure Si we do not mean a bare proton in pure Si; the notation is a mere shorthand for the fact that one electron is left out of the system.³⁵ The other electrons are still allowed to distribute themselves self-consistently

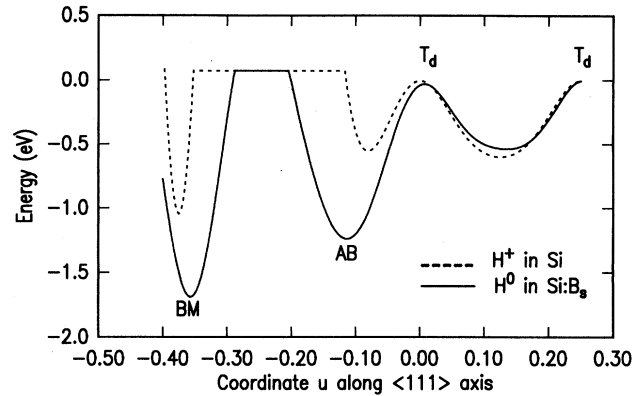


FIG. 4. Energy for positions of the hydrogen atom along the $\langle 111 \rangle$ axis for H⁺ in pure Si (dashed line) and for H⁰ in Si:B (solid line). For all positions of the H atom, coordinates of the host-crystal atoms have been relaxed to minimize the energy. The curves have been truncated at 0.08 eV for positions very close to the Si (in pure Si) or B atom (in Si:B) at $u = -0.25$. The smaller truncated region for B reflects that H can approach the B atom closer than the Si atom.

according to Schrödinger's equation. The line connecting two bonded atoms we call the $\langle 111 \rangle$ axis and the position along this line is given by the single coordinate u ; a coordinate u means that the position has Cartesian coordinates (u, u, u) in units of the Si diamond-structure lattice constant of 5.43 Å. A coordinate $u = -0.5$ denotes the unrelaxed Si atomic position, $u = -0.25$ the unrelaxed B atomic position, and $u = 0$ and 0.25 are *T_d* sites. The comparison with H⁺ in pure Si is the most meaningful comparison that one can make, because H behaves as a donor in *p*-type material and will give up its electron to annihilate the free holes resulting from the ionized acceptor. (This does *not* imply that H behaves as a bare proton everywhere in *p*-type Si; just as for H at the bond-center position in pure Si,³⁵ in the H-B complex the missing electron is not removed from the immediate neighborhood of the H atom, but from a region extending past the neighboring atoms.) The two curves have been obtained from the energy surfaces for the two cases (H⁺ in Si and H in Si:B) by extracting the energy values for coordinates along the $\langle 111 \rangle$ axis. The energy scales have been aligned at the distant *T_d* site, $u = 0.25$. It is clear from Fig. 4 that the influence of the substitutional B atom does not stretch out further than $u = -0.03$, corresponding to 2.1 Å from the B atom. Beyond that point the curves coincide to within better than 0.1 eV (which is about the estimated error of energy calculation and fit together). The above observation justifies the use of symmetrized plane waves with the periodicity of the 8-atom (conventional) unit cell of the diamond structure as basis functions for the expansion of the energy surface. We repeat (see Sec. III E) that this observation does not imply that it is sufficient to do the total-energy calculations in a supercell of eight atoms. This procedure for the expansion of the energy surface is satisfactory if one is interested in this surface in the neighborhood of the B atom (see Sec. II E). Further away from the B atom, the surface is identical to the one for H⁺ in pure Si (see Fig. 4; we have also established this for H positions that are not on the $\langle 111 \rangle$

axis). Figure 4 also shows that B acts as an attractor to the H atom, since the bond-centered and antibonding minima are lowered and moved towards the B atom. From the three-dimensional and contour plots of the energy surface in the complete (110) plane containing the $\langle 111 \rangle$ axis (to be discussed below with Figs. 5 and 6), it follows that the *BM* site is an actual (and even global) minimum, whereas the *AB* site represents a saddle point. There is no energy barrier between the *AB* site and an equivalent *BM* site that is not located along this $\langle 111 \rangle$ axis.

In Figs. 5(a) and 5(b) we show three-dimensional plots of the energy surface for H in Si:B for positions of H in the (110) plane (containing a chain of atoms as in Fig. 3) and the (111) plane through three bond-minima sites, respectively. Figure 5(a) shows the low-energy region (in red) around the B atom. The region does not contain the *AB* and *BB* sites on both extensions of the Si—B bond; these sites appear as saddle points of the energy surface. From Fig. 5(b) it is clear that the low-energy region extends all around the B atom, which is located slightly out of the (111) plane, which is shown in Fig. 5(b).

In Fig. 6(a) we show a contour plot of the energy surface for H in the (110) plane in Si:B. It shows most of the salient features of the complete energy surface, which cannot be shown in one picture since the energy is a function of three independent coordinates. The *BM* site is the global minimum, whereas we see again that the *AB* site is a saddle point. In Fig. 6(b) we show exactly the same part of the energy surface for the case of H^+ in pure Si. From the comparison we see that the H atom gets trapped close to the B atom and has no low-energy pathway to migrate away from the B atom. The H atom can move between equivalent *BM* sites around the B atom by passing over an energy barrier close to the *C* site (between the *C* site and the B atom) of only 0.2 eV. Of course, for this to happen the relaxation of the host crystal has to adjust accordingly. There is no barrier between the *BM* and *C* sites. The low-energy barrier implies that at room temperature the H atom will be able to move around the B atom between the four equivalent *BM* sites. Very recently, in experiments using the optical dichroism of the H-B absorption bands under uniaxial stress, an activation energy of 0.19 eV was found for H motion from one *BM* site to another.²⁴ This activation energy is in excellent agreement with our calculated barrier of 0.2 eV.

We find that the *BM* site is 0.48 eV lower than the *AB* site and 0.29 eV lower than the *C* site. The energy difference between *BM* and *AB* sites of 3.12 eV, obtained in Ref. 14 from Hartree-Fock calculations, we consider to be very unreliable. A final observation from Fig. 6(a) is that the *C* and *C'* sites, which are completely equivalent in pure Si, are not only symmetrically inequivalent (e.g., *C* is at 1.36 Å from the B atom, *C'* at 1.92 Å), but that they differ in energy by the large amount of 1.2 eV. This site inequivalence in the neighborhood of a substitutional impurity leads us to a brief discussion of the accuracy with which ion-channeling experiments are able to determine the site of hydrogen.^{18,20} The analysis of ion-channeling experiments involves a statistical average over the possible substitutional sites for the impurity B atom.⁵⁰

After such an average, the energy surface for a H atom in Si:B has the complete symmetry of the diamond structure of pure Si. This implies that, for instance, the *C* and *C'* sites are considered to be completely equivalent in the analysis of ion-channeling experiments. The same holds for the *AB* and *BB* sites (see Fig. 3), which in our calcula-

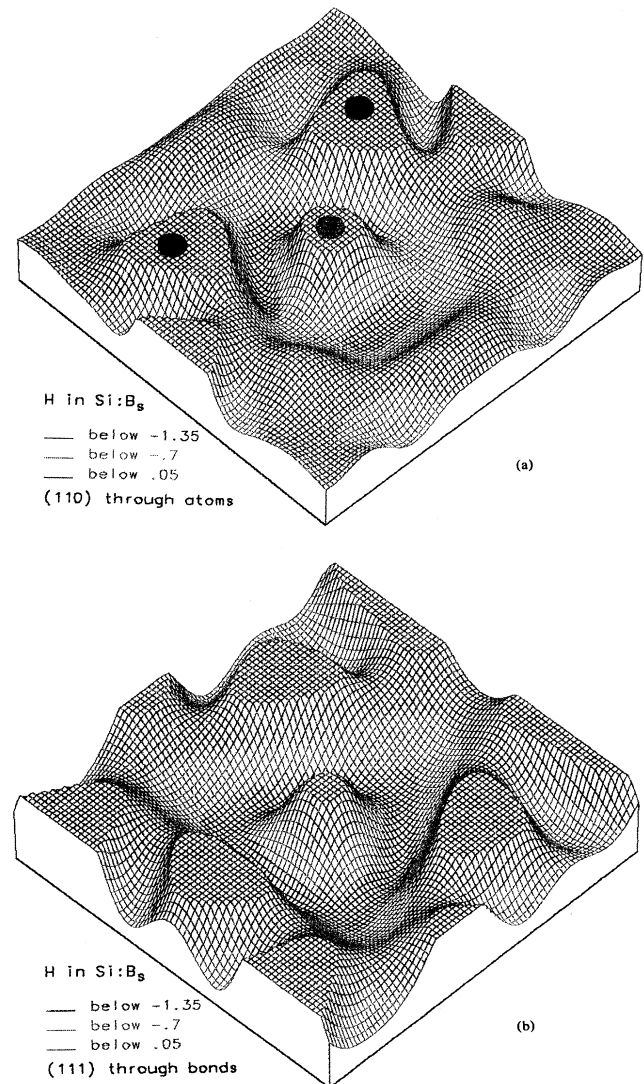


FIG. 5. Energy surface for a hydrogen atom in Si with one substitutional boron atom in (a) a (110) plane containing a chain of atoms, and (b) a (111) plane through three equivalent bond-minima (*BM*) positions. The black dots represent Si atoms and the pink dot the B atom. The plane in (b) does not contain atoms, but the unrelaxed lattice position of the B atom is located just 0.4 Å outside the plane in the center of the surface. Atoms are shown at their unrelaxed positions since they relax differently for different positions of the H atom, but relaxations are taken into account in the total-energy calculations. The energy is below -1.35 eV in the red region, between -1.35 and -0.7 eV in the blue region, and between -0.7 and 0.05 eV in the green region. The surface is cut off at an energy value of 0.05 eV. The zero of energy is chosen at the tetrahedral interstitial site.

tion differ by about 0.7 eV in energy (the *AB* site being the lower-energy site). Therefore, ion-channeling experiments are able to discriminate between sites that remain inequivalent when averaging over the possible substitutional sites for the B atom, e.g., *BM* and *AB* sites. They

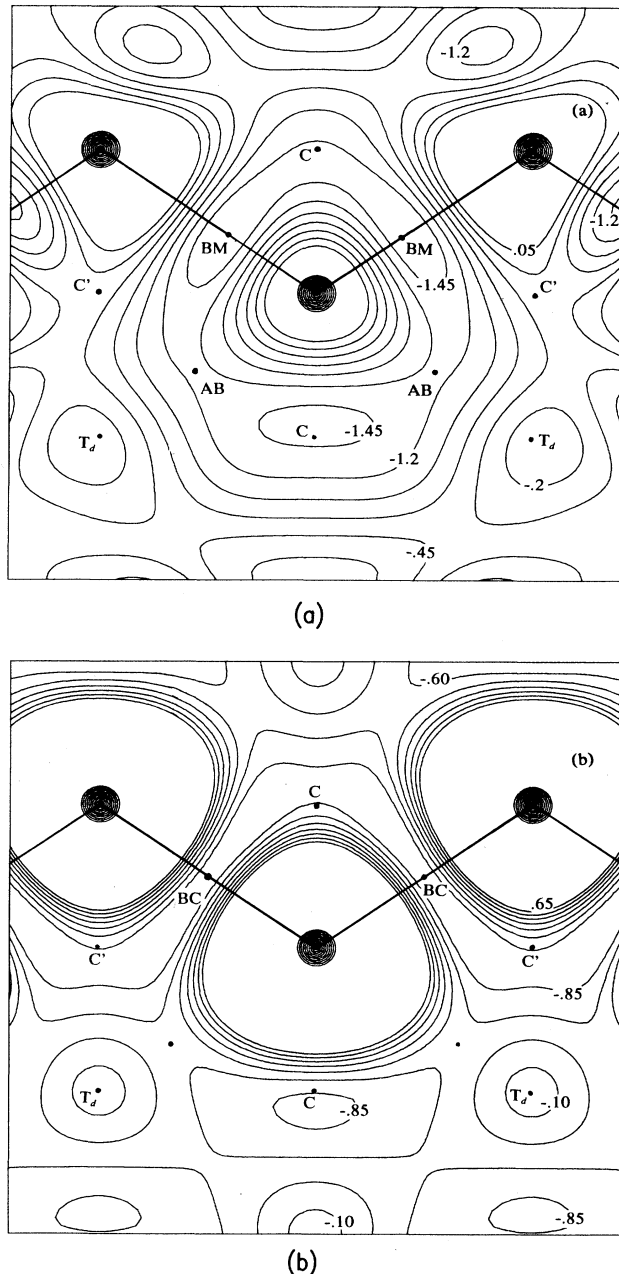


FIG. 6. Contour plots of the energy surface of a H atom in the (110) plane in boron-doped and pure silicon. Large dots indicate (unrelaxed) atomic positions; bonded atoms are connected by solid lines. Positions of special interest are indicated (cf. Fig. 3). The unit of energy is eV and the spacing between contours is 0.25 eV. Close to the atoms contours are not shown above a certain energy value. (a) H^0 in Si:B. The boron atom occupies the center of the plot. Highest contour shown is 0.05 eV. (b) H^+ in pure Si. Highest contour shown 0.65 eV.

cannot discriminate, however, between, e.g., *AB* and *BB* sites. On account of this, the conclusion from these experiments that H resides predominantly in a Si—B bond (a Si—Si bond can be excluded since a large displacement from the substitutional site of the B atom is also observed¹⁸) is indisputable, but the further detailing of percentages of H at other sites²⁰ is not necessarily relevant to the microscopic structure of the H-B complex. Observation in ion-channeling experiments of H at other sites is most likely related to defects which may be located far away from the B atom.

In Fig. 7 we present contour plots of the energy surface in a few other planes, showing that the *BM* site is indeed the global energy minimum and that there is a spherical shell-like region (with some holes in it) at a radial distance of about 1.3 Å from the B atom, for which the energy is between -1.45 and -1.7 eV (with respect to the energy at a far T_d site). Thus the H atom can move around adiabatically on this shell with an energy barrier at a site closer to the C site of only 0.2 eV.

D. Hydrogen vibrational frequencies

Because infrared measurements of the hydrogen vibrational frequency have been an important source of experimental information on the H-B complex,^{4,15,16} it is worthwhile to make a connection with that work by calculating the vibrational frequency for the H-stretching mode. We have done this for a number of different sites for the H atom that all have been proposed as the equilibrium site for the H atom on account of theoretical calculations.

The sites for which we calculated the frequency of the H-stretching mode are the *BM* and *AB* sites already discussed extensively above, as well as the backbonding (*BB*) site shown in Fig. 3. For H in the latter site, the H—Si distance is again 1.60 Å, while the Si atom closest to H relaxes toward the B atom by 0.3 Å. For each of the three sites, we determine the minimum-energy configuration by allowing up to eight atoms around the H atom as well as the H atom itself to relax. Subsequently, we move the H atom away from its equilibrium position in directions corresponding to a stretching mode over distances of 2% and 4% of a Si—Si bond length. The relaxation of the host crystal is now kept as in the minimum-energy configuration.⁵¹ The procedure described above induces energy changes of typically up to 30 meV. These energy differences ΔE are fitted to a parabola $\Delta E = \frac{1}{2} f u_H^2$, where u_H is the displacement of the H atom and f the force constant of the stretching mode. If f is expressed in units of $\text{eV}/\text{Å}^2$, the wave number κ for the stretching mode is given in units of cm^{-1} by

$$\kappa = \frac{1}{2\pi} \left[\frac{f(\text{eV}/\text{Å}^2)}{938.25} \right]^{1/2} \times 10^5 \text{ cm}^{-1}, \quad (4)$$

where we have taken the vibrating object to be a proton (with rest mass $m_p c^2 = 938.25$ MeV). A very similar procedure to the one described here was used successfully by Kaxiras and Joannopoulos⁵² to calculate vibrational frequencies of H atoms saturating dangling bonds at Si and Ge (111) surfaces.

In Table III we summarize our results and list the results of previous theoretical calculations using a variety of methods. From varying the number of calculated points used in the parabolic fit and from calculations at lower energy cutoffs, we estimate the error bar on our calculated frequencies to be 100 cm^{-1} . Also, results ob-

tained from the same calculations in a 16-atom cell fall within this error bar. Considering the error bar, our result for the H vibrational frequency at the *BM* site is in fair agreement with the low-temperature (5 K) experimental results^{16,17} of 1903 and 1907 cm^{-1} . The agreement with the result obtained at 273 K (1870 cm^{-1}) (Ref.

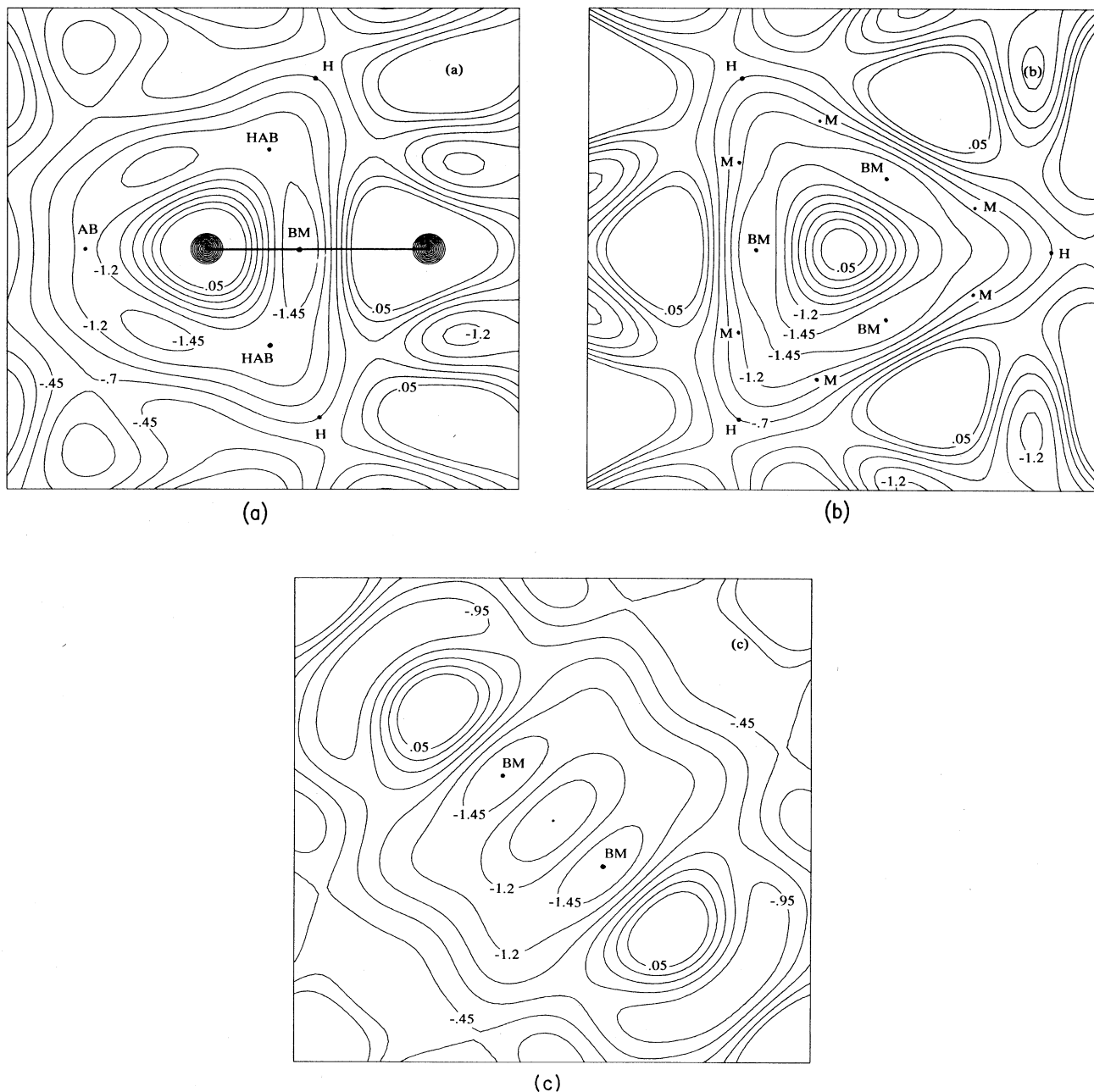


FIG. 7. Contour plots of the energy surface of a neutral H atom in various planes in Si:B [see Fig. 6(a) for the (110) plane]. Indicators are the same as in Fig. 6. (a) (211) plane containing one B—Si bond (B atom on the left). *HAB* denotes the hexagonal antibonding site, a saddle point of the energy surface about halfway between the hexagonal interstitial site *H* and the B atom. (b) (111) plane through three bond minima (*BM* sites). The *M* sites lie halfway between two *C* sites, one of which is in the (110) plane (see Figs. 3 and 6). In this plane there is a ringlike low-energy region around the B atom (that is not located in this plane). The perspective plot for this plane is shown in Fig. 5(b). (c) (001) plane through two bond minima (*BM* sites). This plane is perpendicular to the (110) plane of Fig. 6(a).

TABLE III. Calculated wave numbers κ_{stretch} (in cm^{-1}) of vibrational frequencies of hydrogen-stretching modes for hydrogen in the bond-minimum (*BM*), antibonding (*AB*), and back-bonding (*BB*) sites in Si:B compared with previous theoretical calculations using a variety of methods.

Site	Present	Previous
	result	theoretical
	κ_{stretch}	calculations
		κ_{stretch}
<i>BM</i>	1830	1880, ^a 1820 ^b
<i>AB</i>	1680	1000, ^b 1870, ^c 2590 ^d
<i>BB</i>	1590	
Expt.	1903 ^e	

^aReference 10.

^bReference 26.

^cReference 11.

^dReference 12.

^eReference 16.

15) is even better, but that is not the appropriate number to compare with.

In view of the error bar of 100 cm^{-1} , the results for the *BM* and *AB* sites are not that different, and would not supply strong enough evidence for one to conjecture that the infrared data exclude the *AB* site as the equilibrium site for H. Previous authors did make this claim on account of their finding that the H vibrational frequency is very different for the *BM* and *AB* sites. The peculiar fact occurred, however, that their results for the *BM* site are in general agreement with experiment, but DeLeo and Fowler¹² find the result for the *AB* site to be much larger (2590 cm^{-1}), whereas Chang and Chadi²⁶ find it to be much smaller (1000 cm^{-1}) than the experimental value. These authors did not discuss the accuracy of their calculated result. We stress that, of course, the *AB* site can be ruled out as the equilibrium site for the H atom because of the fact that it is a saddle point of the energy surface and 0.48 eV higher in energy than the *BM* site, without a barrier between the two sites [see Fig. 6(a)]. The result for the *AB* site of 1870 cm^{-1} in Ref. 11 was obtained by fitting a force-constant model to the experimental value that was known at that time. Not too much value must be attached to this result.

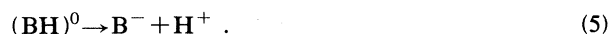
It is interesting to compare our results of Table III with the vibrational frequency for H^0 (H^+) in a BC site (geometrical bond center) in pure Si. For that case we calculate a frequency of 1945 (2210 cm^{-1}). This is much larger than the result for the *BB* site in Table III. Since the frequency for the *BM* site is in between those obtained for a H atom close to one Si atom (at the *BB* site in Si:B) and a H atom in between two Si atoms (at the BC site in Si), we infer that at the *BM* site there is still a fair amount of bonding between H and B besides the bonding between H and Si. The fact that the H atom is also bonded to the B atom (which is a modification of the original description of the bond-centered configuration by Pankove *et al.*⁴) can also be inferred from the fact that the H atom can easily move around the B atom between equivalent *BM* sites, as discussed in the preceding subsection.

Infrared frequencies that have been associated with stretching modes involving a single H atom in hydrogenated amorphous Si and hydrogenated crystalline Si range between 2000 and 2200 cm^{-1} .^{53,54} The fact that our results of 1945 and 2210 cm^{-1} (for H^0 and H^+ at the bond-centered site in pure Si, respectively) are close to these frequencies and also to the vibrational frequency of H saturating a dangling bond at a Si (111) surface (2085 cm^{-1}) is remarkable. We also observe that the *AB*-site frequency of 1680 cm^{-1} resulting from a stretching H—B bond is apparently greatly modified with respect to frequencies of 2560 cm^{-1} (for terminal H bonding) and 1985 cm^{-1} (for bridge bonding) found in diborane.⁴

To conclude this subsection we briefly discuss the side bands in the infrared transmission spectra that were recently found for the H-Al and H-Ga complexes in Si (for the H-B complex the side bands are not resolved, but they are expected to be there).¹⁶ Stavola *et al.*¹⁶ suggested that these side bands are the result of a low-frequency excitation, for which they proposed two possibilities. The first possibility is the tunneling of H between different but equivalent *BM* sites. This must be considered unlikely, because of the rather large adjustments in the relaxation of the host crystal that have to happen for these sites to be indeed equivalent. This explanation was more recently abandoned by Stavola and co-workers.²⁴ The second possibility is that the H atom resides slightly off the *BM* site and off the $\langle 111 \rangle$ axis; the vibration would then be modeled by that of a quasilinear molecule, which is known to have side bands.⁵⁵ In that case, the configuration would resemble that of oxygen bridging a Si—Si bond.⁵⁶ We have investigated this possibility by positioning the H atom slightly off axis from the *BM* site on the $\langle 111 \rangle$ axis. While keeping the relaxation of the surrounding crystal fixed, the energy remained constant for small displacements ($< 0.1 \text{ \AA}$) of the H atom in several directions. We did not allow the surrounding crystal to adjust its relaxation, but this can only lower the energy. However, by moving the H atom off axis, we change the symmetry of the system considerably, and the changes in energy that we obtain fall within the accuracy of our calculations. We conclude that an off-axis position for the H atom is very well possible, but cannot be quantitatively assessed by our calculations.

E. Dissociation energy of the H-B complex

It is found experimentally that at temperatures above 150°C the conductivity of the passivated samples starts to recover and can eventually be restored completely.^{4,5} It seems natural to attribute the increase in conductivity to the dissociation of the H-B complexes and subsequent diffusion of H out of the passivated region. As we saw earlier, H-induced passivation arises from compensation followed by pair formation. By the same token, one can consider the dissociation reaction:



This reaction, however, produces no free holes (i.e., the material is still compensated) and leaves open the possibility of reformation of the pairs by the reverse reaction.

Restoration of the conductivity requires an additional reaction, for instance,



where h^+ denotes a free hole. Reaction (6), which denotes an electronic process, equilibrates very fast. The relative amounts of H^+ versus H^0 are determined by the position of the Fermi level. If the conditions are such that H^0 is overwhelmingly favored over H^+ , the following reaction would apply:



Since B is a shallow acceptor, we can assume that its preferred state (after dissociation of the H-B complex) is an ionized B^- .

We see that there is no unique, single reaction describing the dissociation of the H-B pair. Nevertheless, we have calculated dissociation energies associated with *specific* dissociation reactions. By dissociation energy we mean the energy difference between the initial and final configurations of the breakup reaction. Quite generally, one can define for any reaction that can occur in two directions the reaction activation energies for the forward and reverse reactions. The dissociation energy as defined above is also precisely the difference between the two reaction activation energies associated with the dissociation reaction.

The dissociation energy associated with reaction (5) is found by calculating the following total energies:⁵¹ (i) $E(\text{HB})$, the total energy of the fully relaxed Si:B crystal with H at the *BM* site; (ii) $E(\text{B}^-)$, the total energy of the fully relaxed Si crystal with a substitutional B^- ; (iii) $E(\text{H}^+)$, the total energy of a fully relaxed Si crystal with a H^+ at the *BC* site; and (iv) $E(\text{Si})$, the total energy of a pure Si crystal. The dissociation energy E_d may now be defined as

$$E_d = -E(\text{HB}) + E(\text{B}^-) + E(\text{H}^+) - E(\text{Si}). \quad (8)$$

This dissociation energy does not depend on the Fermi level, because no electrons or holes are involved in reaction (5). This formula results in $E_d = 0.59$ eV.

To calculate the dissociation energy based on reaction (7), one has to use the following formula:

$$E_d = -E(\text{HB}) + E(\text{B}^-) + E(\text{H}^0) + E(h^+) - E(\text{Si}), \quad (9)$$

where $E(h^+)$ is the energy of a free hole, for which we take minus the Fermi energy E_F (a hole is the absence of an electron). The dissociation energy in (9) does depend on the Fermi level because it involves reaction (6). From (9) we find a dissociation energy $E_d = 1.09$ eV $- E_F$.

Experimentally, one can determine a dissociation energy if the dissociation is governed by first-order kinetics, i.e., the rate of change with time of the number of pairs N is proportional to N :

$$\frac{dN}{dt} = -\nu N, \quad (10)$$

where ν is the dissociation rate constant. This assumption would have to be tested by demonstrating a linear

dependence of $\ln(N)$ on time for several temperatures [$\ln(N) = -\nu t$]. For ν , an Arrhenius-type temperature dependence is usually assumed:

$$\nu = \nu_0 e^{-E_A/kT}, \quad (11)$$

where ν_0 is an attempt frequency and E_A the activation energy. If the assumption of first-order kinetics holds, the measured temperature dependence of ν allows one to extract the activation energy E_A . This activation energy is the energy barrier that must be overcome for the breakup to occur [for instance, the forward-reaction activation energy of reaction (5)]. It *does not* correspond to a dissociation energy in the sense of the energy difference between the pair and the isolated breakup products.

The experimental procedure just described has not been carried out. Wichert *et al.*²² followed the simplified procedure of isochronal annealing in which they *assumed* first-order kinetics. They extracted an activation energy of 1.3 eV in the case of H-In pairs. They estimated that the H-B pairs would break up with a smaller activation energy. We note, however, that it has been found⁵⁷ that first-order kinetics is not obeyed, so that this number may not be particularly meaningful and cannot be compared with theoretical values. A more sophisticated analysis of the data would be needed to extract energies that can be compared with theory.

Finally, we mention that one may define the binding energy of the H-B complex as the difference between the energy of the H-B complex in a Si crystal and the sum of the energies of a (neutral) H atom in free space and of a (neutral) B substitutional in Si. This binding energy is more of a conceptual quantity, contrary to the dissociation energy discussed above (which, however, is often called a binding energy as well). According to this definition a binding energy of 3.31 eV is obtained.⁵⁸

IV. CONCLUSIONS

The study of the total-energy surface for H in Si:B using the first-principles pseudopotential-density-functional method presented in this paper conclusively shows that a H-B complex is formed in which the H atom occupies a site close to the center of a Si—B bond (*BM* site). This complex is the net result of the passivation mechanism that removes the shallow-acceptor level from the gap, thereby neutralizing the electrical activity of boron-doped silicon. Other sites that were previously proposed to be equilibrium sites for H by others are shown to be saddle points of the energy surface that are higher in energy by at least 0.48 eV. We find that the H atom can move between four equivalent *BM* sites over a spherical shell-like region with an energy barrier of only 0.2 eV.

The calculated vibrational frequency for the H-stretching mode centered on the *BM* site is in good agreement with infrared and Raman experiments. The occurrence of sidebands in the infrared spectrum can be qualitatively understood since H can reside slightly off the bond axis from the *BM* site.

ACKNOWLEDGMENTS

This work was supported in part by the U.S. Office of Naval Research under Contract No. N00014-84-C-0396.

One of us (P.J.H.D.) acknowledges support from IBM Netherlands N.V. We further acknowledge useful discussions with Dr. A. D. Marwick.

- *Present address: Physics Department, University of Nijmegen, Toernooiveld, 6525 ED Nijmegen, The Netherlands.
- †Present address: Philips Laboratories, 345 Scarborough Road, Briarcliff Manor, NY 10510.
- ¹S. J. Pearton, J. W. Corbett, and T. S. Shi, *Appl. Phys. A* **43**, 153 (1987).
- ²An overview of recent work may be found in *Defects in Electronic Materials*, Materials Research Society Symposia Proceedings Vol. 104, edited by M. Stavola, S. J. Pearton, and G. Davies (Materials Research Society, Pittsburgh, PA, 1988), pp. 229–309.
- ³C. T. Sah, J. Y. C. Sun, and J. J. T. Tzou, *Appl. Phys. Lett.* **43**, 204 (1983); *J. Appl. Phys.* **54**, 5864 (1983).
- ⁴J. I. Pankove, D. E. Carlson, J. E. Berkeyheiser, and R. O. Wance, *Phys. Rev. Lett.* **51**, 2224 (1983); J. I. Pankove, R. O. Wance, and J. E. Berkeyheiser, *Appl. Phys. Lett.* **45**, 1100 (1984); J. I. Pankove, P. J. Zanzucchi, and C. W. Magee, *ibid.* **46**, 421 (1985).
- ⁵N. M. Johnson and M. D. Moyer, *Appl. Phys. Lett.* **46**, 787 (1985); N. M. Johnson, *Phys. Rev. B* **31**, 5525 (1985).
- ⁶N. M. Johnson, C. Herring, and D. J. Chadi, *Phys. Rev. Lett.* **56**, 769 (1986); **59**, 2116 (1987); N. M. Johnson and C. Herring, in *Defects in Electronic Materials*, Materials Research Society Symposia Proceedings Vol. 104, edited by M. Stavola, S. J. Pearton, and G. Davies (Materials Research Society, Pittsburgh, PA, 1988), p. 277.
- ⁷K. Bergman, M. Stavola, S. J. Pearton, and J. Lopata, *Phys. Rev. B* **37**, 2770 (1988).
- ⁸S. T. Pantelides, *Appl. Phys. Lett.* **50**, 995 (1987).
- ⁹C. G. Van de Walle, Y. Bar-Yam, and S. T. Pantelides, *Phys. Rev. Lett.* **60**, 2761 (1988).
- ¹⁰G. G. DeLeo and W. B. Fowler, *Phys. Rev. B* **31**, 6861 (1985).
- ¹¹L. V. C. Assali and J. R. Leite, *Phys. Rev. Lett.* **55**, 980 (1985); **56**, 403 (1986).
- ¹²G. G. DeLeo and W. B. Fowler, *Phys. Rev. Lett.* **56**, 402 (1986).
- ¹³J. M. Baranowski and J. Tatarkiewicz, *Phys. Rev. B* **35**, 7450 (1987).
- ¹⁴A. Amore Bonapasta, A. Lapicciarella, N. Tomassini, and M. Capizzi, *Phys. Rev. B* **36**, 6228 (1987).
- ¹⁵M. Stavola, S. J. Pearton, J. Lopata, and W. C. Dautremont-Smith, *Appl. Phys. Lett.* **50**, 1086 (1987).
- ¹⁶M. Stavola, S. J. Pearton, J. Lopata, and W. C. Dautremont-Smith, *Phys. Rev. B* **37**, 8313 (1988).
- ¹⁷M. Stutzmann, *Phys. Rev. B* **35**, 5921 (1987); M. Stutzmann and C. P. Herrero, *Appl. Phys. Lett.* **51**, 1413 (1987).
- ¹⁸A. D. Marwick, G. S. Oehrlein, and N. M. Johnson, *Phys. Rev. B* **36**, 4539 (1987).
- ¹⁹A. D. Marwick, G. S. Oehrlein, J. H. Barrett, and N. M. Johnson, in *Defects in Electronic Materials*, Materials Research Society Symposia Proceedings Vol. 14, edited by M. Stavola, S. J. Pearton, and G. Davies (Materials Research Society, Pittsburgh, PA, 1988), p. 259.
- ²⁰B. B. Nielsen, J. U. Andersen, and S. J. Pearton, *Phys. Rev. Lett.* **60**, 321 (1988).
- ²¹Th. Wichert, H. Skudlik, H.-D. Carstanjen, T. Enders, M. Deicher, G. Grübel, R. Keller, L. Song, and M. Stutzmann, in *Defects in Electronic Materials*, Materials Research Society Symposia Proceedings Vol. 104, edited by M. Stavola, S. J. Pearton, and G. Davies (Materials Research Society, Pittsburgh, PA, 1988), p. 265.
- ²²Th. Wichert, H. Skudlik, M. Deicher, G. Grübel, R. Keller, E. Recknagel, and L. Song, *Phys. Rev. Lett.* **59**, 2087 (1987).
- ²³M. Stutzmann, J. Harsanyi, A. Breitschwerdt, and C. P. Herrero, *Appl. Phys. Lett.* **52**, 1667 (1988).
- ²⁴M. Stavola, K. Bergman, S. J. Pearton, and J. Lopata, *Phys. Rev. Lett.* **61**, 2786 (1988).
- ²⁵P. Deák, L. C. Snyder, R. K. Singh, and J. W. Corbett, *Phys. Rev. B* **36**, 9612 (1987); P. Deák and L. C. Snyder, *ibid.* **36**, 9619 (1987).
- ²⁶K. J. Chang and D. J. Chadi, *Phys. Rev. Lett.* **60**, 1422 (1988).
- ²⁷P. Hohenberg and W. Kohn, *Phys. Rev.* **136**, B864 (1964); W. Kohn and L. J. Sham, *ibid.* **140**, A1133 (1965).
- ²⁸D. R. Hamann, M. Schlüter, and C. Chiang, *Phys. Rev. Lett.* **43**, 1494 (1979).
- ²⁹J. Perdew and A. Zunger, *Phys. Rev. B* **23**, 5048 (1981).
- ³⁰D. M. Ceperley and B. J. Alder, *Phys. Rev. Lett.* **45**, 566 (1980).
- ³¹J. Ihm, A. Zunger, and M. L. Cohen, *J. Phys. C* **12**, 4409 (1979).
- ³²P. J. H. Denteneer, Ph.D. thesis, Eindhoven University of Technology, 1987, available from the author upon request.
- ³³S. G. Louie, in *Electronic Structure, Dynamics, and Quantum Structural Properties of Condensed Matter*, edited by J. T. Devreese and P. E. van Camp (Plenum, New York, 1985).
- ³⁴Y. Bar-Yam, S. T. Pantelides, and J. D. Joannopoulos, *Phys. Rev. B* **39**, 3396 (1989).
- ³⁵C. G. Van de Walle, P. J. H. Denteneer, Y. Bar-Yam, and S. T. Pantelides, the preceding paper, *Phys. Rev. B* **39**, 10 791 (1989).
- ³⁶R. M. Wentzcovitch, M. L. Cohen, and P. K. Lam, *Phys. Rev. B* **36**, 6058 (1987).
- ³⁷P. O. Löwdin, *J. Chem. Phys.* **19**, 1396 (1951).
- ³⁸G. B. Bachelet, D. R. Hamann, and M. Schlüter, *Phys. Rev. B* **26**, 4199 (1982).
- ³⁹Two special points (see Refs. 43 and 44) are used in these calculations to integrate over the first Brillouin zone.
- ⁴⁰F. D. Murnaghan, *Proc. Nat. Acad. Sci. U.S.A.* **30**, 244 (1944).
- ⁴¹*Landolt-Börnstein: Numerical Data and Functional Relationships in Science and Technology*, edited by O. Madelung, M. Schulz, and H. Weiss (Springer, Berlin, 1982), Gp. 3, Vol. 17, Pt. a.
- ⁴²Y. Bar-Yam and J. D. Joannopoulos, *Phys. Rev. B* **30**, 1844 (1984).
- ⁴³A. Baldereschi, *Phys. Rev. B* **7**, 5212 (1973); D. J. Chadi and M. L. Cohen, *ibid.* **8**, 5747 (1973).
- ⁴⁴H. J. Monkhorst and J. D. Pack, *Phys. Rev. B* **13**, 5188 (1976).
- ⁴⁵M. S. Hybertsen and S. G. Louie, *Phys. Rev. B* **34**, 5390 (1986); R. W. Godby, M. Schlüter, and L. J. Sham, *ibid.* **37**, 10 159 (1988).
- ⁴⁶J. A. Vergés, D. Glötzel, M. Cardona, and O. K. Andersen, *Phys. Status Solidi B* **113**, 519 (1982).

- ⁴⁷K. Shih, W. E. Spicer, W. A. Harrison, and A. Sher, *Phys. Rev. B* **31**, 1139 (1985).
- ⁴⁸E. A. Kraut and W. A. Harrison, *J. Vac. Sci. Technol. B* **3**, 1267 (1985).
- ⁴⁹L. S. Bartell and B. L. Carroll, *J. Chem. Phys.* **40**, 1135 (1965).
- ⁵⁰J. H. Barrett, *Phys. Rev. B* **3**, 1527 (1971).
- ⁵¹These calculations were done in a 32-atom cell with energy cutoffs of (10;20) Ry and two special \mathbf{k} points.
- ⁵²E. Kaxiras and J. D. Joannopoulos, *Phys. Rev. B* **37**, 8842 (1988).
- ⁵³M. H. Brodsky, M. Cardona, and J. J. Cuomo, *Phys. Rev. B* **16**, 3556 (1977).
- ⁵⁴H. J. Stein, *Phys. Rev. Lett.* **43**, 1030 (1979).
- ⁵⁵W. R. Thorson and I. Nakagawa, *J. Chem. Phys.* **33**, 994 (1960).
- ⁵⁶D. R. Bosomworth, W. Hayes, A. R. L. Spray, and G. D. Watkins, *Proc. R. Soc. London, Ser. A* **317**, 133 (1970).
- ⁵⁷M. Stavola (private communication).
- ⁵⁸Since the crystal calculations do not include spin-polarization effects, we calculate the energy of the H atom also without spin polarization. Our calculated number is quantitatively rather unreliable since a calculation in a crystal is compared with an atomic calculation and these are very different regarding approximations that are made. This is illustrated by the fact that if the two crystal calculations are performed with the lower cutoffs (6;12) Ry [as opposed to (10;20) Ry for the quoted value], the binding energy becomes 2.75 eV.

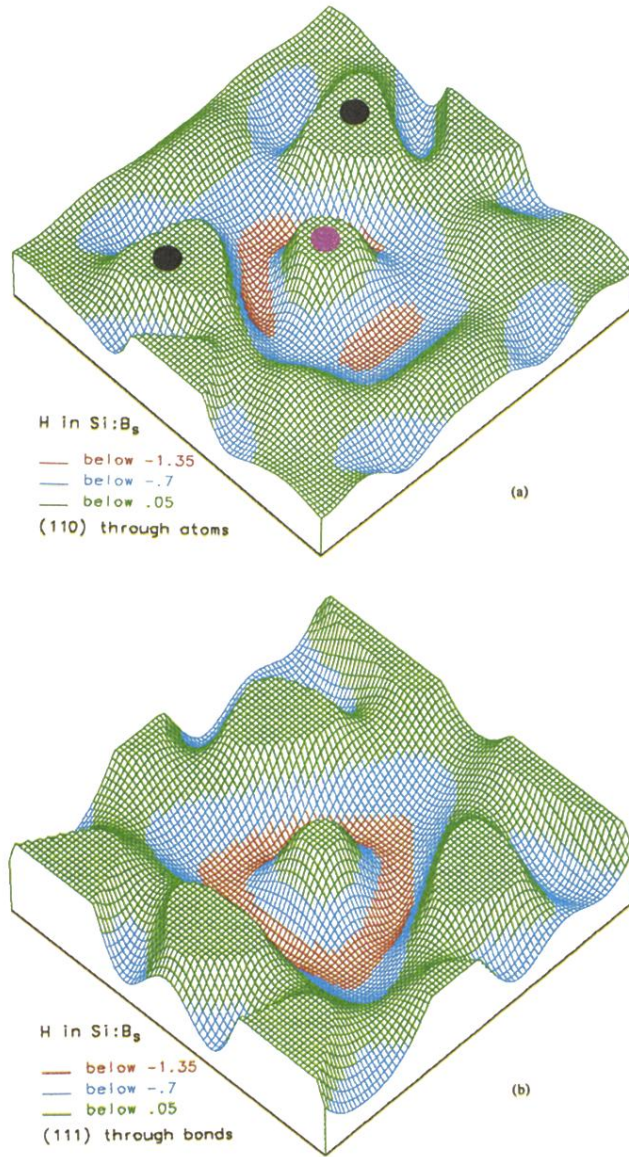


FIG. 5. Energy surface for a hydrogen atom in Si with one substitutional boron atom in (a) a (110) plane containing a chain of atoms, and (b) a (111) plane through three equivalent bond-minima (*BM*) positions. The black dots represent Si atoms and the pink dot the B atom. The plane in (b) does not contain atoms, but the unrelaxed lattice position of the B atom is located just 0.4 \AA outside the plane in the center of the surface. Atoms are shown at their unrelaxed positions since they relax differently for different positions of the H atom, but relaxations are taken into account in the total-energy calculations. The energy is below -1.35 eV in the red region, between -1.35 and -0.7 eV in the blue region, and between -0.7 and 0.05 eV in the green region. The surface is cut off at an energy value of 0.05 eV . The zero of energy is chosen at the tetrahedral interstitial site.